

Review

# Identifying and Manipulating Giant Vesicles: Review of Recent Approaches

Taro Toyota <sup>1,2,\*</sup> and Yiting Zhang <sup>1</sup>

<sup>1</sup> Department of Basic Science, Graduate School of Arts and Sciences, The University of Tokyo, 3-8-1 Komaba, Meguro-ku, Tokyo 153-8902, Japan; zy-si@g.ecc.u-tokyo.ac.jp

<sup>2</sup> Universal Biology Institute, The University of Tokyo, 3-8-1 Komaba, Meguro-ku, Tokyo 153-8902, Japan

\* Correspondence: cttoyota@mail.ecc.u-tokyo.ac.jp

**Abstract:** Giant vesicles (GVs) are closed bilayer membranes that primarily comprise amphiphiles with diameters of more than 1  $\mu\text{m}$ . Compared with regular vesicles (several tens of nanometers in size), GVVs are of greater scientific interest as model cell membranes and protocells because of their structure and size, which are similar to those of biological systems. Biopolymers and nano-/microparticles can be encapsulated in GVVs at high concentrations, and their application as artificial cell bodies has piqued interest. It is essential to develop methods for investigating and manipulating the properties of GVVs toward engineering applications. In this review, we discuss current improvements in microscopy, micromanipulation, and microfabrication technologies for progress in GV identification and engineering tools. Combined with the advancement of GV preparation technologies, these technological advancements can aid the development of artificial cell systems such as alternative tissues and GV-based chemical signal processing systems.

**Keywords:** giant vesicle; micromanipulation; microscopy; microfluidic device



**Citation:** Toyota, T.; Zhang, Y. Identifying and Manipulating Giant Vesicles: Review of Recent Approaches. *Micromachines* **2022**, *13*, 644. <https://doi.org/10.3390/mi13050644>

Academic Editors: Ryuji Kawano, Kosuke Ino, Daisuke Kiriya, Hiroaki Onoe and Masahiro Takinoue

Received: 19 March 2022

Accepted: 17 April 2022

Published: 19 April 2022

**Publisher's Note:** MDPI stays neutral with regard to jurisdictional claims in published maps and institutional affiliations.



**Copyright:** © 2022 by the authors. Licensee MDPI, Basel, Switzerland. This article is an open access article distributed under the terms and conditions of the Creative Commons Attribution (CC BY) license (<https://creativecommons.org/licenses/by/4.0/>).

## 1. Introduction

Chemical sciences that mimic biological processes aim to improve our understanding of the exceptional molecular recognition and efficient molecular conversion capabilities of proteins, in addition to the mechanism of information conversion achieved by DNA and RNA. Supramolecular and systems chemistry [1] has led to substantial advancements in these studies. Artificial cells based on cell-sized molecular aggregates [2] have been actively produced in recent years to imitate cellular functions.

Giant vesicles (GVs) have drawn attention as one of the cell-sized molecular self-assemblies [3]. GV is a molecular self-assembly composed of amphiphilic molecules forming a closed bilayer membrane in which the hydrophobic parts face each other in water and has a size greater than or equal to 1  $\mu\text{m}$ . The self-assembled bilayer and cell membranes have equivalent main constituents, the phospholipids. Because of this, GVVs have attracted scientific attention as a chemical model of cells.

When vesicles are composed of phospholipids, which are the primary components of the cell membrane, they are labeled liposomes [4]. Vesicles that comprise synthesized amphiphilic macromolecules are called polymersomes [5]. Some papers describe liposomes and polymersomes with diameters of 1  $\mu\text{m}$  or more as “giant liposomes” and “giant polymersomes”, respectively [6,7]. Moreover, based on structural appearance (Figure 1), GVVs have been categorized as giant unilamellar vesicles (GUVs) made of a single bilayer membrane and giant multilamellar vesicles (GMVs) that have a nested structure or multiple membranes. Benefiting from the development of microfabrication technologies, GV preparation methods have made great strides in the last 20 years [3]. In particular, because GUVs are more likely to encapsulate biopolymers and nano-/microparticles than GMV [8], many studies have been conducted on supramolecular chemistry for understanding cellular dynamics and functions using GUVs. For example, GUV-based sensors, processors, and

actuators equipped with proteins, DNA, and RNA, have been invented [9–13]. Moreover, GVs that can cause proliferation of the membrane itself upon membrane precursors have also been reported [14–18].

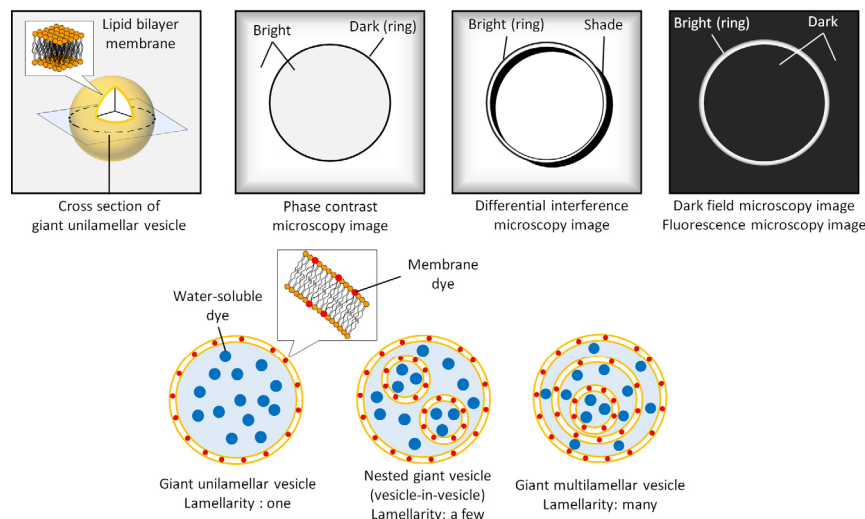


**Figure 1.** Schematic illustration of giant vesicles and their cross-sectional images in different kinds of microscopic technologies.

To increase the level of GV functions aimed at the hierarchy of cellular functions, it is important to increase the structural hierarchy of GVs. The assembly of GVs has attracted attention as a basis for highly functionalized supramolecular chemical systems. In assembling technology for GVs, it is indispensable to determine the kind of GV to be assembled and identify each of the GVs. Therefore, in this review, we introduce the recent identification and characterization methods of GV and the progress of the manipulation methods developed by microfabrication technology. In addition, we discuss the process of constructing GV-based cell mimicry devices with higher-order functions.

## 2. Identification Methods of GVs

### 2.1. Morphology

GVs have diameters of 1  $\mu\text{m}$  or greater and can be observed in situ without staining or fixing under an optical microscope due to the difference between the refractive index of the membrane and that of water. Conventional research on GVs has aimed to clarify the mechanism of cell shape using GVs as cell models, and thus, microscopic observation has been an important identification method for GV morphology (Figure 1). For example, a nested giant vesicle is characterized as a “vesicles-in-vesicle” configuration like eucaryotic cells. Individual observations of GVs are mostly performed by using phase-contrast, dark-field, or differential interference contrast microscopy. A phase-contrast microscope is used to observe GVs with a small number of vesicular membranes, resulting in fewer halos in the microscopy images. Dark-field microscopy completely shuts out the transmitted light around the vesicular membrane. As a result, it is possible to observe a single vesicular membrane with a thickness of approximately 5 nm. In contrast, differential interference microscopy has the advantage of not only observing GUVs, but also GMVs. The stained GVs are similarly observed under a bright-field microscope. GVs can encapsulate water-soluble dyes and colored particles that can be observed under a bright-field microscope. However, it is difficult to observe the vesicular membrane with ordinary hydrophobic dyes because of the interference of ambient transmitted light. Therefore, fluorescence microscopy, in which the ambient transmitted light is completely shut out, is a powerful tool for observing GVs. Additionally, confocal laser scanning fluorescence microscopy provides higher spatial resolution than epifluorescence microscopy and has become popular for GV

observation among researchers. An automated algorithm for GV structural assessment using confocal laser scanning fluorescence microscopy images was developed by García-Sáez's group [19]. More recently, Dimova's group developed observation techniques for GUVs based on stimulated emission depletion (STED) microscopy, which can provide a high spatial resolution beyond the diffraction limit of light [20,21]. They found that the deduced membrane spontaneous curvature of nanometer-sized vesicular tubes produced from GVs, was in excellent agreement with theoretical predictions.

Although detailed optical microscopy observation of individual GVs is effective for scrutinizing the GV structural morphology, it is difficult to statistically and quantitatively evaluate the morphologies of large amounts of GV. Flow cytometry has been used to measure the GV population. While Vorauer-Uhl et al. first reported the flow cytometric evaluation of the size distribution of nanometer-sized fluorescence-labeled vesicles [22], Yomo's group investigated the structural properties of large amounts of GVs [23]. The group used fluorescent proteins, such as green fluorescent protein, to evaluate the inner water volume of individual GVs. Fluorescence-labeled phospholipids were used to determine the lipid membrane volume via the thickness and surface area of the phospholipids. Additionally, they reported a structural comparison of GVs prepared using different methods [24,25]. It was found that the water-oil-emulsion templating method [26] for the preparation of GUVs can provide a large number of GVs with apparently unilamellar vesicular membranes, where the nominal number of bilayer membranes contained in the individual GV was found to be 2–3.

## 2.2. Lamellarity

Lamellarity of GV is defined as the number of bilayer membranes contained in individual GVs. The film swelling method, which is a standard preparation method for GVs, usually affords a mixture of GUVs (with a lamellarity of 1) and GMVs (with a maximum lamellarity of several thousand). The recent development of GV preparation methods, including the water-oil-emulsion templating method, enables GUV production and the encapsulation of water-soluble molecules and particles into GUVs [3]. A membrane permeation experiment using a membrane-penetrating protein,  $\alpha$ -hemolysin [27], has become the standard method for determining whether GV observed under the microscope has a lamellarity of one [28].  $\alpha$ -Hemolysin is a channel-type membrane protein and composed of a hydrophobic part that recognizes and enters the lipid bilayer membrane and a hydrophilic part of several nanometers. When added to GVs,  $\alpha$ -hemolysin pierces the outermost vesicular membrane from the outside and does not move into the interior. Therefore, if a water-soluble fluorescent molecule is encapsulated inside the GV and its lamellarity is one, the encapsulated molecule permeates and diffuses to the outside of the GV through the pores of the  $\alpha$ -hemolysin. Recently, de novo designed transmembrane pores of proteins or DNA origami have also been reported by several groups [29,30].

A quantitative attempt to evaluate GV lamellarity was recently performed by Ishiwata's group [31]. The group carefully observed individual GVs labeled by fluorescent phospholipids (the number of assessed GVs was over 200) and plotted the mean fluorescence intensities of GVs along the circumference against the GV diameter. They found that the plot showed discrete distributions and could be classified into several groups. The GV group with fluorescence intensities similar to the predicted value of the ideal GUV and few dependencies on size were assigned to the GUV. They found that several fluorescent dyes for the vesicular membrane of GVs could affect the lamellarity of GVs produced by the water-in-oil emulsion templating method. By fitting a model to differential interference contrast microscopy images, McPhee et al. measured the lamellarity of GVs and validated the data by comparison with epifluorescence microscopy images [32]. This approach is important in terms of label-free measurements, which excludes the inherent drawbacks of fluorescent labeling such as sample modification and photobleaching.

### 2.3. Membrane Bending Rigidity

The membrane bending rigidity or membrane modulus of GV is one of the most important characteristic parameters that have been measured historically in many studies from the biophysical viewpoint of cell membranes. Many measurement studies have been conducted to observe vesicular membrane deformation caused by the suction of a glass capillary (micropipette) under a microscope [33]. The micropipette assay of GVs also enables the measurement of the viscosity of the vesicular membrane by oscillatory shear gradient [34]. A microfluidic device that can fold and aspirate a GV in a narrow space, called an on-chip micropipette, has been developed [35]. Recently, an electroporation technique was applied for membrane tension measurement as well as line tension measurement because GV deformation and rupture are regulated by electroporation conditions [36]. However, the micropipette is brought into contact with a GV and a direct force is applied as a perturbation to the vesicular membrane; thus, physical interference has sometimes been regarded as a perturbation (plastic deformation) in these methods [37]. Therefore, as a non-contact and non-perturbative measurement, observing a wavy motion mode, called fluctuation, has been conducted. This fluctuation of the GV membrane occurs due to the random collision of water molecules and is used to calculate the membrane bending rigidity [38–40]. After the fluctuations of the GV membrane around an equilibrium shape are monitored, Fourier decomposition of the contours is applied, and the mean square values of the shape deviations are determined.

In addition, visualization of membrane bending rigidity using fluorescent dyes for GV membranes has been developed (Figure 2). A specific pair of fluorescent molecules can change their fluorescence intensity through Förster resonance energy transfer (or fluorescence resonance energy transfer), which reflects the distance between the molecules shifted by bending the vesicular membrane [41]. Recently, Roux's group observed that a hydrophobic dithienothiophene derivative, FliptR (fluorescent lipid tension reporter), buried in the vesicular membrane, can change excitation maxima and fluorescence lifetime responding to the membrane tension and rigidity [42]. The group successfully visualized not only GV membrane tension but also that of cell membranes using FliptR.

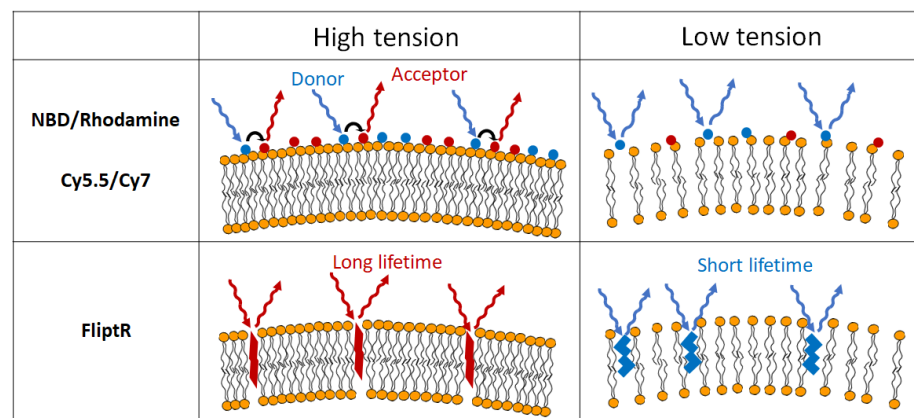


**Figure 2.** Schematic illustration of visualizing membrane tension by fluorescent membrane dyes.

### 2.4. Permeability and Intramembrane Ion Current

As explained previously, the membranes of GVs are semipermeable, that is, water-soluble molecules with large molecular weights and ions scarcely permeate the membrane, while water molecules can permeate. Membrane permeability is another important physical parameter for measuring GVs through cell membranes. A single GUV observation for membrane permeation of encapsulated water-soluble fluorescence dyes under a microscope is repeatedly and quantitatively performed to determine the reliability of the permeation rate. Yamazaki's group applied this method to clarify the mechanism of bioactive substances, such as magainin 2, which interacts with cell membranes to enhance membrane permeation

upon chemical stimulus of such substances [43]. The apparatus for membrane permeation measurement was equipped with a glass capillary that gently added a substance in the vicinity of the GVs. In recent years, after trapping GVs in cup-shaped microstructures fabricated in microfluidic devices, researchers have examined GV membrane permeation under a fluorescence microscope upon exposure to bioactive substances such as  $\alpha$ -hemolysin. [44]. Sugiyama et al. recently reported that exposure to water-soluble fluorescent molecules such as uranine, results in their accumulation inside GVs against their concentration gradient under a steady flow [45,46]. Their evaluation of this unusual phenomenon indicated the possibility of asymmetric distribution of phospholipids between the inner and outer leaflets of GVs when the GVs are exposed to a steady flow.

The ion current of the GV membrane has drawn attention in the construction of model nerve cells based on GVs. The physiological measurement of ion currents in the nerve cell membrane, called the patch-clamp technique, also enables us to measure those in the GV membrane. Hamada et al. and Fukuda et al. independently applied the whole-cell patch-clamp technique to measure the ion currents of GV membranes inserted with membrane proteins [47,48]. Velasco-Olmo et al. reported that the whole-cell patch-clamp method can be applied for the lamellarity assessment of GV membranes generated on spherical objects [49].

### 2.5. Other Properties

Other properties of vesicles, such as the zeta potential and heat of transition of the vesicular membrane, are significant physical properties in terms of not only the model cell membrane, but also the drug delivery carrier. These properties have been measured for nanometer-sized vesicles because such vesicles, called small or large vesicles (<1000 nm), can be uniform through ultrasonication and filtration [50,51]. However, to the best of our knowledge, there is no report on a methodology that enables the measurement of the zeta potential or the heat of transition of individual GV. One reason for this is that conventional preparation methods for GVs are not optimized to produce GVs with uniform sizes, structures, and properties. Recent advances in GV preparation methods to provide GUVs of uniform size [52] will solve this problem. Another solution is the development of a micro-apparatus for electrophoretic mobility and calorimetric measurements using microelectrodes and thermocouples that can stably sweep the electric field. Because such microfabricated apparatus has already been applied to measure the properties of single cells [53], they will be used to single GV measurements.

## 3. Manipulation Methods of GVs

### 3.1. Immobilization on a Substrate

The more detailed the observation of each GV under a high-resolution optical microscope, the longer the observation time. This sometimes causes difficulties in capturing 3D images of individual GVs owing to Brownian motion or membrane fluctuation. The current technical problem has been solved through the development of high-speed scanning confocal laser fluorescence microscopy [54] and light-sheet fluorescence microscopy [55]. However, the importance of establishing a method that can immobilize GVs on a substrate for detailed observation has increased.

A commonly used method is to modify GVs with biotin-tagged phospholipids. This results in GVs that are heavier than their surroundings, which settle onto a substrate coated with avidin. For example, encapsulation of sucrose inside GVs and addition of same osmolarity glucose on the outside [56]. In contrast, Cuvelier et al. reported avidin-coated GVs immobilized on a substrate modified with biotin-tagged casein [57]. They observed a GV response under shear stress in the flow field, due to the strong interaction of biotin-avidin bonds. In addition to biotin-avidin interaction, there were reports that the linker between GVs and the substrate is DNA [58] or protein (integrin) [59]. Because the bilayer membrane is likely to get wet on a flat substrate, it is necessary to pay attention to the practice of GV immobilization. The settled GVs can rupture on the substrate and transform

into a bilayer membrane film [60]. To avoid such rupture, GUVs can be buried in an agarose gel at concentrations of 0.25–0.5% *w/v*. Lira et al. observed that the lateral displacement of GUVs in agarose gels was completely suppressed [61].

### 3.2. Size Sorting and Purification

The preparative technology for GVs has advanced not only in controlling lamellarity but also in fabricating uniform sizes [52,62,63]. In some devices, there are constraints on the lipid composition, applicable buffered solution, and flow field; as a result, it is not always possible to prepare monodispersed GVs under general-purpose experimental conditions. Therefore, size-sorting methods for GVs of various sizes are desirable. Several groups have reported GV size sorting (called purification) using filters [64–66]. All groups filtered the GV dispersion using membrane filters made of polycarbonate, where the pores size ranged from 3  $\mu\text{m}$  to 12  $\mu\text{m}$ . Each group remarked that gentle extrusion is important for the purification process.

In addition, size sorting techniques for GVs using microfluidic devices have recently been proposed following cell sorting microfluidic technology [67]. Kazayama et al. reported that deterministic lateral displacement (DLD) is a promising mechanism for GV size sorting (Figure 3a). This is carried out by evaluating the DLD for GV dispersion with a microfluidic device and integrating the DLD and region of trapping microstructures [68]. They achieved monodisperse trapped GVs with a variation coefficient of approximately 10%. Robinson's group also suggested a size-sorting microfluidic mechanism with massive trapping of GVs by devising a trapping structure [69]. Recently, using the stream bifurcation structure of a microfluidic device, GV purification, which separates GUVs from a mixture of GUVs and additives (including nanometer-sized particles), was performed by a pinched-flow fractionation mechanism (Figure 3b) [70].

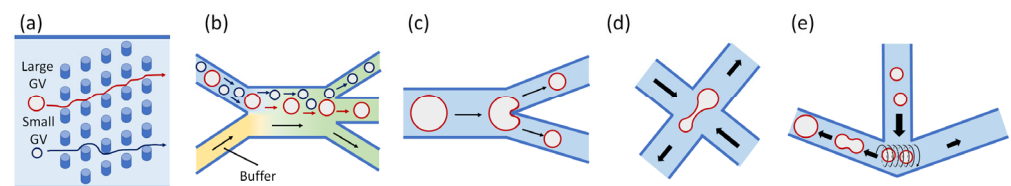


**Figure 3.** Schematic illustrations of microfluidic devices for size sorting, purification, and manipulation: (a) deterministic lateral displacement, (b) pinched-flow fractionation, (c) Y-junction for splitting GVs, (d) cross-road for holding and stretching GVs, and (e) anchor-shape junction for vesicle fusion.

### 3.3. Microfluidic Manipulation

The trapping and morphological change induction of GVs by hydrodynamic fields have become popular in microfluidic device development as well as the GV preparation method. As already mentioned, GVs are likely to be captured by simply pouring the GV dispersion into a microfluidic device equipped with cup-shaped microstructures with a narrow gap. Ditrich's group developed a device that created a curtain of air bubbles around each GV-trapping microstructure to protect the trapped GV from the surrounding flow field [44]. Yamada et al. reported that GV can be trapped and purified by a well-type space with a gap in the vertical direction [71].

The advantage of using microfluidic devices is that, owing to the development of materials and hydrodynamic methodologies for microfluidic devices, it is possible to freely design shapes and pour GV dispersions for observation and manipulation. For instance, by devising the shape of the trapping structure, Schwille's group held to trap the prolate-shaped GVs and found a novel pattern formation of the encapsulated protein, FtsZ, that self-assembles in response to the GV shape [72]. Dekker's group developed a microfluidic device that could induce GV splitting (Figure 3c) [73]. Kumar et al. manufactured a crossroad-type microfluidic device to trap and deform GV in the center (Figure 3d) [74]. Stone's group developed a microfluidic device that causes a vortex at a junction and found

that vesicle fusion occurs there (Figure 3e) [75]. Lira et al. observed the binding and fusion of nanometer-sized vesicles on GV membranes with different surface charges [76]. Sen's group reported microfluidic devices that can evaluate liposomes propelled by enzymatic reactions on liposomal surfaces [77]. These innovations will continue to stimulate the development of artificial cell systems.

### 3.4. Micropipette Manipulation

As mentioned above, measurement of the membrane bending rigidity of GVs is conventionally performed using a glass capillary as a micropipette. Micropipette aspiration can hold them and allow morphological changes in GVs. When the tip of the micropipette is sufficiently narrower than the GV and the suction pressure is sufficiently strong, the GV membrane stretches to form a tubular structure [78]. Furthermore, in two micropipette systems that enable the holding of one GV at each tip of the micropipettes, the adhesion between the two GVs can be evaluated by bringing the GVs close to each other via micropipette manipulation (Figure 4a).

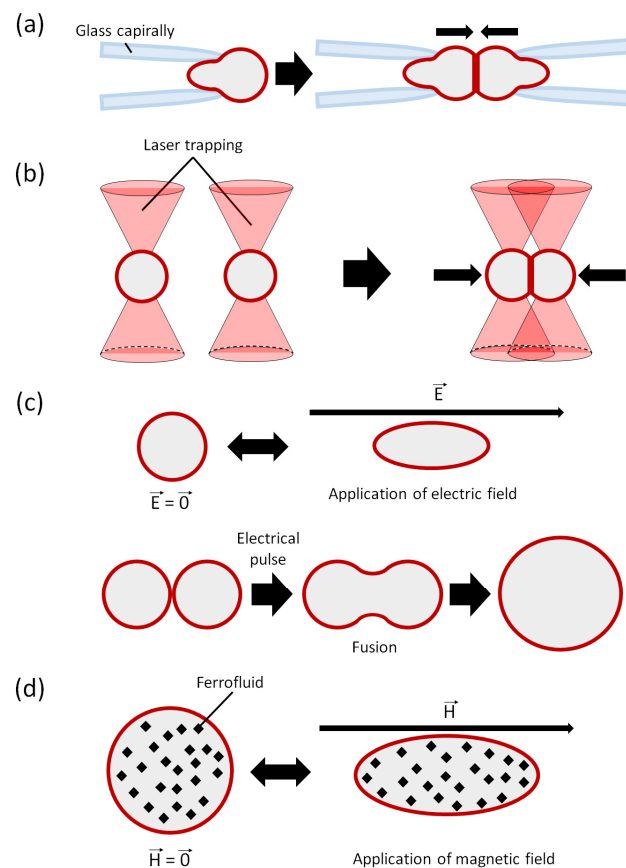


**Figure 4.** Schematic illustration of manipulation of GVs by (a) glass capillary (micropipette), (b) optical tweezers, (c) electric field, and (d) magnetic field (for GVs encapsulating ferrofluid).

Orwar's group extended the micropipette technique to morphological changes in GVs [79]. The group established a glass capillary with a microelectrode inside, which is often used in the patch-clamp technique to measure intramembrane ion currents. They placed the glass capillary near a GV, together with the counter electrode and found that when an electric field was applied, part of the GV membrane could be stretched and transformed into a tubular structure, and then attached to the tip of the glass capillary. They showed that by adjusting the electric field voltage, the tip of the tubular membrane is led to adhere to an adjacent GV, and the GVs were connected to exchange the internal aqueous solution [80]. In contrast, Lobovkina's group reported that by applying positive

pressure toward the inside of the GUV at the contact tip of a micropipette, a string-bead structure made of a stretched GV membrane was produced inside the GUV [81]. In addition, microinjection is also possible with a micropipette by piercing a part of the GV membrane with a tip with a diameter of 1  $\mu\text{m}$  [82–84].

### 3.5. Optical Trapping and Acoustic Trapping

Laser technology has advanced research in the scientific and engineering fields, and the optical tweezers (or laser trapping) have had a great impact on GV manipulation. In the initial research on optical tweezers on GVs, the transformation of GVs was observed due to the light radiation pressure of a laser applying a GV membrane, which has a higher refractive index than water [85,86]. GVs encapsulated in an inner aqueous solution with a high refractive index can be carried by moving the stage while the GVs are trapped or by moving the laser focus [87,88]. When a microbead is held by an optical tweezer and brought into contact with the GV membrane, a nanometer-sized tubular structure is formed by pulling the microbead [21]. Inaba et al. examined membrane stretching using microbeads that were suspended and shifted using an optical tweezer inside of a GV [89]. Taking advantage of the fact that optical tweezers exert various effects on GVs, Elani's group successfully collected multiple GUVs with optical tweezers, brought them into contact with each other, and further pierced them to execute a sequential enzymatic reaction inside the partially fused GVs (Figure 4b) [90]. Shiomi et al. developed a platform that can repeat the fusion and division of GVs using a combination of optical tweezers, electroporation, and temperature stimulation [91]. Recently, Yoshino et al. showed that a sub-micrometer-sized vesicle could be captured and transported by a gradient of the force of light evanescent waves along an optical nanofiber [92].

GV manipulation is also realized using sound pressure. The advantage of sound waves is irradiation variation, that is, squeezing sound pressure in a relatively small area or creating a periodic pattern of sound pressure in a limited space. In the former case, pore formation in the GV membrane occurs [93]. In the latter case, different types of GVs in a mixed dispersion can be sorted by composition, owing to the difference in the sound pressure response [94]. A collaboration between Mann and Drinkwater's group revealed that GVs gathered and were forced to deform under an acoustic pressure field [95,96]. Interestingly, Pereno et al. revealed that a vortex stream occurs inside GUVs when they are exposed to ultrasound pressure [97].

### 3.6. Electric and Magnetic Field Application

The electric and magnetic fields directly affect the properties of the lipid molecules, so that GV manipulation, including shape change of GVs, is easily performed (Figure 4c). The electroporation of GV is the most popular phenomenon, as mentioned above. Moreover, by arranging the application condition of voltages, it is possible to keep GVs with a hole of several micrometers in diameter or to keep them in an angular shape that is not observed in the equilibrium state [98–100]. In contrast, dielectrophoresis leads to GVs gathering; hence, GVs can be fused by controlling the application of an electric field [101,102]. Nomura and Morishima's group have independently reported that GV was fused with cells by dielectrophoresis [103,104]. By preparing and mixing two types of GVs with different dielectrophoresis responses and applying an alternating electric field to the mixture dispersion, the frequency shift for dielectrophoresis successfully sorted them into two groups [105]. When GUVs are irradiated by microwaves, which are electromagnetic waves, the difference in their microwave transmittance depends on the membrane composition [106]. This approach is expected to be a new non-contact GV manipulation technique.

GVs respond to a magnetic field that is a result of diamagnetic susceptibility of the lipid bilayer membrane. Historically, Helfrich's first report on GV morphology suggested the perturbation of GV shapes by a magnetic field [107]. Recently reports showed the fusion and fission of vesicles were induced by strong magnetic field application [108]. Suzuki et al. reported that tubular GVs composed of phospholipids and collagen, which have

the anisotropic diamagnetic susceptibility different from that of phospholipid membranes, form a specific curved structure (called *elastica*) in response to a high magnetic field [109]. In contrast, Bacri et al. showed that GVs containing superparamagnetic nanoparticles, that is, ferrofluid, are deformed by a weak magnetic field (Figure 4d) [110]. Liposomes encapsulating such nanoparticles are called magnetoliposomes and have drawn considerable attention as novel drug delivery carriers [111]. Nomura's group reported that cell-sized magnetoliposomes can be remotely controlled and manipulated by an external magnetic field [112]. Han's group demonstrated the assembly of magnetoliposomes by an external magnetic field. They also observed that chemical reactions of magnetoliposomes, including glucose oxidase and a transmembrane pore peptide, melittin, which can produce H<sub>2</sub>O<sub>2</sub> inducing cell death in the vicinity of the assembly (GUV colony) under glucose exposure [113].

### 3.7. Laser-Assisted Three-Dimensional (3D) Printing Inside of GUV

3D printing technology has sparked a revolution in the micro-construction of molds for fundamental material research and industrial applications [114]. One of the most eye-catching features of this technology is that 3D printing is based on digital fabrication technologies. Thus, through computational design, the construction of molecular aggregate in a 3D manner is practically and reproducibly controlled. Göpfrich's group developed a two-photon laser-assisted 3D printing technology inside GUVs [115,116]. They constructed tubular 3D molds not only inside but also in the intramembrane of GUV and the membrane permeability of the GUV was changed by the mold. This emerging technique opens future manufacturing and tuning of artificial cells.

## 4. Summary

In this paper, we review recent developments in GV identification and manipulation methods and summarize the advantages of basic techniques for assembling GVs as building blocks. Several approaches overlap with cell manipulation techniques. However, GVs have no cytoskeleton or cell wall and therefore require careful handling of their physical properties. Imminent enhanced development of artificial cell construction is expected due to these methods, leading to the construction of elaborate artificial tissues and information processing systems composed of GVs [95,113,117,118].

**Author Contributions:** Writing-original draft preparation, T.T.; writing-review and editing, T.T. and Y.Z.; visualization, Y.Z. All authors have read and agreed to the published version of the manuscript.

**Funding:** This research was partly funded by a Grant-in-Aid for Transformative Research Areas "Molecular Cybernetics" (to T.T.; Grant 20H05969) from the Ministry of Education, Culture, Sports, Science and Technology, Japan.

**Conflicts of Interest:** The authors declare no conflict of interest.

## References

1. Ashkenasy, G.; Hermans, T.M.; Otto, S.; Taylor, A.F. Systems chemistry. *Chem. Soc. Rev.* **2017**, *46*, 2543–2554. [[CrossRef](#)] [[PubMed](#)]
2. Chang, T.M.S. Artificial cells with emphasis on bioencapsulation in biotechnology. *Biotech. Ann. Rev.* **1995**, *1*, 267–295.
3. Dimova, R.; Stano, P.; Marques, C.M.; Walde, P. Preparation methods for giant unilamellar vesicles. In *The Giant Vesicle Book*; Dimova, R., Marques, C.M., Eds.; CRC Press: Boca Raton, FL, USA, 2020; pp. 3–16.
4. Sessa, G.; Weissmann, G. Phospholipid spherules (liposomes) as a model for biological membranes. *J. Lipid Res.* **1968**, *9*, 310–318. [[CrossRef](#)]
5. Discher, B.M.; Won, Y.Y.; Ege, D.S.; Lee, J.C.; Bates, F.S.; Discher, D.E.; Hammer, D.A. Polymersomes: Tough vesicles made from diblock copolymers. *Science* **1999**, *284*, 1143–1146. [[CrossRef](#)]
6. Criado, M.; Keller, B.U. A membrane fusion strategy for single-channel recordings of membranes usually non-accessible to patch-clamp pipette electrodes. *FEBS Lett.* **1987**, *224*, 172–176. [[CrossRef](#)]
7. Discher, B.M.; Won, Y.Y.; Ege, D.S.; Lee, J.M.; Bates, F.S.; Discher, D.E.; Hammer, D.A. Cellular mimics engineered from diblock copolymers. In Proceedings of the First Joint BMES/EMBS Conference: 1999 IEEE Engineering in Medicine and Biology 21st Annual Conference and the 1999 Annual Fall Meeting of the Biomedical Engineering Society, Atlanta, GA, USA, 13–16 October 1999; Volume 1, p. 75.

8. Tanaka, S.; Takiguchi, K.; Hayashi, M. Repetitive stretching of giant liposomes utilizing the nematic alignment of confined actin. *Commun. Phys.* **2018**, *1*, 18. [[CrossRef](#)]
9. Lach, S.; Yoon, S.M.; Grzybowski, B.A. Tactic, reactive, and functional droplets outside of equilibrium. *Chem. Soc. Rev.* **2016**, *45*, 4766–4796. [[CrossRef](#)]
10. Sato, Y.; Takinoue, M. Creation of artificial cell-like structures promoted by microfluidics technologies. *Micromachines* **2019**, *10*, 216. [[CrossRef](#)]
11. Robinson, T. Microfluidic handling and analysis of giant vesicles for use as artificial cells: A review. *Adv. Biosyst.* **2019**, *3*, 1800318. [[CrossRef](#)]
12. Lyu, Y.; Peng, R.; Liu, H.; Kuai, H.; Mo, L.; Han, D.; Li, J.; Tan, W. Protocells programmed through artificial reaction networks. *Chem. Sci.* **2020**, *11*, 631–642. [[CrossRef](#)]
13. Olivi, L.; Berger, M.; Creyghton, R.N.; De Franceschi, N.; Dekker, C.; Mulder, B.M.; Claassens, N.J.; ten Wolde, P.R.; van der Oost, J. Towards a synthetic cell cycle. *Nat. Commun.* **2021**, *12*, 4531. [[CrossRef](#)]
14. Stano, P.; Luisi, P.L. Semi-synthetic minimal cells: Origin and recent developments. *Curr. Opin. Biotechnol.* **2013**, *24*, 633–638. [[CrossRef](#)] [[PubMed](#)]
15. Mann, S. Systems of creation: The emergence of life from nonliving matter. *Acc. Chem. Res.* **2012**, *45*, 2131–2141. [[CrossRef](#)] [[PubMed](#)]
16. Adamala, K.; Szostak, J.W. Competition between model protocells driven by an encapsulated catalyst. *Nat. Chem.* **2013**, *5*, 495–501. [[CrossRef](#)] [[PubMed](#)]
17. Kurihara, K.; Tamura, M.; Shohda, K.-I.; Toyota, T.; Suzuki, K.; Sugawara, T. Self-reproduction of supramolecular giant vesicles combined with the amplification of encapsulated DNA. *Nat. Chem.* **2011**, *3*, 775–781. [[CrossRef](#)] [[PubMed](#)]
18. Podolsky, K.A.; Devaraj, N.K. Synthesis of lipid membranes for artificial cells. *Nat. Rev. Chem.* **2021**, *5*, 676–694. [[CrossRef](#)]
19. Hermann, E.; Bleicken, S.; Subburaj, Y.; García-Sáez, A.J. Automated analysis of giant unilamellar vesicles using circular Hough transformation. *Bioinformatics* **2014**, *30*, 1747–1754. [[CrossRef](#)] [[PubMed](#)]
20. Zhao, Z.; Roy, D.; Steinkühler, J.; Robinson, T.; Lipowsky, R.; Dimova, R. Super-Resolution Imaging of Highly Curved Membrane Structures in Giant Vesicles Encapsulating Molecular Condensates. *Adv. Mater.* **2022**, *34*, 2106633. [[CrossRef](#)]
21. Roy, D.; Steinkühler, J.; Zhao, Z.; Lipowsky, R.; Dimova, R. Mechanical Tension of Biomembranes Can Be Measured by Super Resolution (STED) Microscopy of Force-Induced Nanotubes. *Nano Lett.* **2020**, *20*, 3185–3191. [[CrossRef](#)]
22. Vorauer-Uhl, K.; Wagner, A.; Borth, N.; Katinger, H. Determination of liposome size distribution by flow cytometry. *Cytometry* **2000**, *39*, 166–171. [[CrossRef](#)]
23. Sato, K.; Obinata, K.; Sugawara, T.; Urabe, I.; Yomo, T. Quantification of structural properties of cell-sized individual liposomes by flow cytometry. *J. Biosci. Bioeng.* **2006**, *102*, 171–178. [[CrossRef](#)] [[PubMed](#)]
24. Nishimura, K.; Hosoi, T.; Sunami, T.; Toyota, T.; Fujinami, M.; Oguma, K.; Matsuura, T.; Suzuki, H.; Yomo, T. Population analysis of structural properties of giant liposomes by flow cytometry. *Langmuir* **2009**, *25*, 10439–10443. [[CrossRef](#)] [[PubMed](#)]
25. Matsushita-Ishiodori, Y.; Hanczyc, M.M.; Wang, A.; Szostak, J.W.; Yomo, T. Using imaging flow cytometry to quantify and optimize giant vesicle production by water-in-oil emulsion transfer methods. *Langmuir* **2019**, *35*, 2375–2382. [[CrossRef](#)]
26. Pautot, S.; Frisken, B.J.; Weitz, D.A. Production of unilamellar vesicles using an inverted emulsion. *Langmuir* **2003**, *19*, 2870–2879. [[CrossRef](#)]
27. Bayley, H. Pore-forming proteins with built-in triggers and switches. *Bioorg. Chem.* **1995**, *23*, 340–354. [[CrossRef](#)]
28. Noireaux, V.; Libchaber, A. A vesicle bioreactor as a step toward an artificial cell assembly. *Proc. Natl. Acad. Sci. USA* **2004**, *101*, 17669–17674. [[CrossRef](#)]
29. Shoji, K.; Kawano, R. Recent advances in liposome-based molecular robots. *Micromachines* **2020**, *11*, 788. [[CrossRef](#)]
30. Xu, C.; Lu, P.; Gamal El-Din, T.M.; Pei, X.Y.; Johnson, M.C.; Uyeda, A.; Bick, M.J.; Xu, Q.; Jiang, D.; Bai, H.; et al. Computational design of transmembrane pores. *Nature* **2020**, *585*, 129–134. [[CrossRef](#)]
31. Chiba, M.; Miyazaki, M.; Ishiwata, S.I. Quantitative analysis of the lamellarity of giant liposomes prepared by the inverted emulsion method. *Biophys. J.* **2014**, *107*, 346–354. [[CrossRef](#)]
32. McPhee, C.I.; Zorinants, G.; Langbein, W.; Borri, P. Measuring the lamellarity of giant lipid vesicles with differential interference contrast microscopy. *Biophys. J.* **2013**, *105*, 1414–1420. [[CrossRef](#)]
33. Karal, M.A.S.; Ahamed, M.K.; Ahmed, M.; Mahbubb, Z.B. Recent developments in the kinetics of ruptures of giant vesicles under constant tension. *RSC Adv.* **2021**, *11*, 29598. [[CrossRef](#)]
34. Fa, N.; Marques, C.M.; Mendes, E.; Schröder, A.P. Rheology of giant vesicles: A micropipette study. *Phys. Rev. Lett.* **2004**, *92*, 108103. [[CrossRef](#)]
35. Elias, M.; Dutoya, A.; Laborde, A.; Lecestre, A.; Montis, C.; Caselli, L.; Berti, D.; Lonetti, B.; Roux, C.; Joseph, P. Microfluidic characterization of biomimetic membrane mechanics with an on-chip micropipette. *Micro Nano Eng.* **2020**, *8*, 100064. [[CrossRef](#)]
36. Portet, T.; Dimova, R. A new method for measuring edge tensions and stability of lipid bilayers: Effect of membrane composition. *Biophys. J.* **2010**, *99*, 3264–3273. [[CrossRef](#)] [[PubMed](#)]
37. Ratanabanangkoon, P.; Gropper, M.; Merkel, R.; Sackmann, E.; Gast, A.P. Mechanics of Streptavidin-Coated Giant Lipid Bilayer Vesicles: A Micropipet Study. *Langmuir* **2003**, *19*, 1054–1062. [[CrossRef](#)]
38. Méléard, P.; Pott, T. Overview of a quest for bending elasticity measurement. *Adv. Planar Lipid Bilayers Liposomes* **2013**, *17*, 55–75.

39. Drabik, D.; Przybyło, M.; Chodaczek, G.; Iglič, A.; Langner, M. The modified fluorescence based vesicle fluctuation spectroscopy technique for determination of lipid bilayer bending properties. *Biochim. Biophys. Acta-Biomembr.* **2016**, *1858*, 244–252. [[CrossRef](#)]
40. Faizi, H.A.; Reeves, C.J.; Georgiev, V.N.; Vlahovska, P.M.; Dimova, R. Fluctuation spectroscopy of giant unilamellar vesicles using confocal and phase contrast microscopy. *Soft Matter* **2020**, *16*, 8996–9001. [[CrossRef](#)]
41. Boyd, M.A.; Kamat, N.P. Visualizing tension and growth in model membranes using optical dyes. *Biophys. J.* **2018**, *115*, 1307–1315. [[CrossRef](#)]
42. Colom, A.; Derivery, E.; Soleimanpour, S.; Tomba, C.; Molin, M.D.; Sakai, N.; González-Gaitán, M.; Matile, S.; Roux, A. A fluorescent membrane tension probe. *Nat. Chem.* **2018**, *10*, 1118–1125. [[CrossRef](#)]
43. Hasan, M.; Yamazaki, M. Elementary Processes and Mechanisms of Interactions of Antimicrobial Peptides with Membranes—Single Giant Unilamellar Vesicle Studies. In *Antimicrobial Peptides*; Matsuzaki, K., Ed.; Springer: Singapore, 2019; pp. 17–32.
44. Robinson, T.; Kuhn, P.; Eyer, K.; Dittrich, P.S. Microfluidic trapping of giant unilamellar vesicles to study transport through a membrane pore. *Biomicrofluidics* **2013**, *7*, 044105. [[CrossRef](#)] [[PubMed](#)]
45. Sugiyama, H.; Osaki, T.; Takeuchi, S.; Toyota, T. Hydrodynamic accumulation of small molecules and ions into cell-sized liposomes against a concentration gradient. *Commun. Chem.* **2020**, *3*, 32. [[CrossRef](#)]
46. Sugiyama, H.; Osaki, T.; Takeuchi, S.; Toyota, T. Role of Negatively Charged Lipids Achieving Rapid Accumulation of Water-Soluble Molecules and Macromolecules into Cell-Sized Liposomes against a Concentration Gradient. *Langmuir* **2022**, *38*, 112–121. [[CrossRef](#)] [[PubMed](#)]
47. Hamada, S.; Tabuchi, M.; Toyota, T.; Sakurai, T.; Hosoi, T.; Nomoto, T.; Nakatani, K.; Fujinami, M.; Kanzaki, R. Giant vesicles functionally expressing membrane receptors for an insect pheromone. *Chem. Commun.* **2014**, *50*, 2958–2961. [[CrossRef](#)] [[PubMed](#)]
48. Fukuda, H.; Nitta, M.; Sakamoto, M.; Shoji, A.; Sugawara, M. Alamethicin Channels as a Signal Transduction Element in an Immobilized Single Giant Unilamellar Vesicle. *Sens. Mater.* **2021**, *33*, 171–180. [[CrossRef](#)]
49. Velasco-Olmo, A.; Ormaetxea Gisasola, J.; Martinez Galvez, J.M.; Vera Lillo, J.; Shnyrova, A.V. Combining patch-clamping and fluorescence microscopy for quantitative reconstitution of cellular membrane processes with Giant Suspended Bilayers. *Sci. Rep.* **2019**, *9*, 7255. [[CrossRef](#)]
50. Biltonen, R.L.; Lichtenberg, D. The use of differential scanning calorimetry as a tool to characterize liposome preparations. *Chem. Phys. Lipids* **1993**, *64*, 129–142. [[CrossRef](#)]
51. Smith, M.C.; Crist, R.M.; Clogston, J.D.; McNeil, S.E. Zeta potential: A case study of cationic, anionic, and neutral liposomes. *Anal. Bioanal. Chem.* **2017**, *409*, 5779–5787. [[CrossRef](#)]
52. Yandrapalli, N.; Petit, J.; Baumchen, O.; Robinson, T. Surfactant-free production of biomimetic giant unilamellar vesicles using PDMS-based microfluidics. *Commun. Chem.* **2021**, *4*, 100. [[CrossRef](#)]
53. Lavaisse, L.M.; Hollmann, A.; Nazareno, M.A.; Disalvo, E.A. Zeta potential changes of *Saccharomyces cerevisiae* during fermentative and respiratory cycles. *Colloids Surf. B Biointerfaces* **2019**, *174*, 63–69. [[CrossRef](#)]
54. Jimbo, T.; Sakuma, Y.; Urakami, N.; Zihlerl, P.; Imai, M. Role of Inverse-Cone-Shape Lipids in Temperature-Controlled Self-Reproduction of Binary Vesicles. *Biophys. J.* **2016**, *110*, 1551–1562.
55. Loftus, A.F.; Noreng, S.; Hsieh, V.L.; Parthasarathy, R. Robust measurement of membrane bending moduli using light sheet fluorescence imaging of vesicle fluctuations. *Langmuir* **2013**, *29*, 14588–14594. [[CrossRef](#)]
56. Sackmann, E. Supported membranes: Scientific and practical applications. *Science* **1996**, *271*, 43–48. [[CrossRef](#)] [[PubMed](#)]
57. Cuvelier, D.; Vezy, C.; Viallat, A.; Bassereau, P.; Nassoy, P. Mimicking cell/extracellular matrix adhesion with lipid membranes and solid substrates: Requirements, pitfalls and proposals. *J. Phys. Condens. Matter* **2004**, *16*, S2427. [[CrossRef](#)]
58. Van Lengerich, B.; Rawle, R.J.; Boxer, S.G. Covalent attachment of lipid vesicles to a fluid-supported bilayer allows observation of DNA-mediated vesicle interactions. *Langmuir* **2010**, *26*, 8666–8672. [[CrossRef](#)] [[PubMed](#)]
59. Guttenberg, Z.; Lorz, B.; Sackmann, E.; Boulbitch, A. First-order transition between adhesion states in a system mimicking cell-tissue interaction. *Europhys. Lett.* **2001**, *54*, 826–832. [[CrossRef](#)]
60. Wang, T.; Ingram, C.; Weisshaar, J.C. Model lipid bilayer with facile diffusion of lipids and integral membrane proteins. *Langmuir* **2010**, *26*, 11157–11164. [[CrossRef](#)]
61. Lira, R.B.; Steinkühler, J.; Knorr, R.L.; Dimova, R.; Riske, K.A. Posing for a picture: Vesicle immobilization in agarose gel. *Sci. Rep.* **2016**, *6*, 25254. [[CrossRef](#)]
62. Misawa, N.; Motegi, T.; Tero, R. Electroformation from patterned single-layered supported lipid bilayers for formation of giant vesicles with narrow size distribution. *Appl. Phys. Express* **2014**, *7*, 117001. [[CrossRef](#)]
63. Ushiyama, R.; Koiwai, K.; Suzuki, H. Plug-and-play microfluidic production of monodisperse giant unilamellar vesicles using droplet transfer across Water–Oil interface. *Sens. Actuators. B Chem.* **2022**, *355*, 131281. [[CrossRef](#)]
64. Karal, M.A.S.; Rahman, M.; Ahamed, M.; Shibly, S.U.A.; Ahmed, M.; Shakil, M. Low-cost non-electromechanical technique for the purification of giant unilamellar vesicles. *Euro. Biophys. J.* **2019**, *48*, 349–359. [[CrossRef](#)]
65. Tamba, Y.; Terashima, H.; Yamazaki, M. A membrane filtering method for the purification of giant unilamellar vesicles. *Chem. Phys. Lipids* **2011**, *164*, 351–358. [[CrossRef](#)]
66. Zhu, T.F.; Szostak, J.W. Preparation of large monodisperse vesicles. *PLoS ONE* **2009**, *4*, e5009. [[CrossRef](#)] [[PubMed](#)]
67. Witek, M.A.; Freed, I.M.; Soper, S.A. Cell separations and sorting. *Anal. Chem.* **2019**, *92*, 105–131. [[CrossRef](#)]
68. Kazayama, Y.; Teshima, T.; Osaki, T.; Takeuchi, S.; Toyota, T. Integrated microfluidic system for size-based selection and trapping of giant vesicles. *Anal. Chem.* **2016**, *88*, 1111–1116. [[CrossRef](#)] [[PubMed](#)]

69. Yandrapalli, N.; Robinson, T. Ultra-high capacity microfluidic trapping of giant vesicles for high-throughput membrane studies. *Lab Chip* **2019**, *19*, 626–633. [[CrossRef](#)] [[PubMed](#)]
70. Tivony, R.; Fletcher, M.; Al Nahas, K.; Keyser, U.F. A microfluidic platform for sequential assembly and separation of synthetic cell models. *ACS Synth. Biol.* **2021**, *10*, 3105–3116. [[CrossRef](#)] [[PubMed](#)]
71. Yamada, A.; Lee, S.; Bassereau, P.; Baroud, C.N. Trapping and release of giant unilamellar vesicles in microfluidic wells. *Soft Matter* **2014**, *10*, 5878–5885. [[CrossRef](#)] [[PubMed](#)]
72. Ganzinger, K.A.; Merino-Salomón, A.; García-Soriano, D.A.; Butterfield, A.N.; Litschel, T.; Siedler, F.; Schwille, P. FtsZ reorganization facilitates deformation of giant vesicles in microfluidic traps. *Angew. Chem. Int. Ed.* **2020**, *59*, 21372–21376. [[CrossRef](#)]
73. Deshpande, S.; Spoelstra, W.K.; Van Doorn, M.; Kerssemakers, J.; Dekker, C. Mechanical division of cell-sized liposomes. *ACS Nano* **2018**, *12*, 2560–2568. [[CrossRef](#)]
74. Kumar, D.; Schroeder, C.M. Nonlinear Transient and Steady State Stretching of Deflated Vesicles in Flow. *Langmuir* **2021**, *37*, 13976–13984. [[CrossRef](#)] [[PubMed](#)]
75. Shin, S.; Ault, J.T.; Stone, H.A. Flow-Driven Rapid Vesicle Fusion via Vortex Trapping. *Langmuir* **2015**, *31*, 7178–7182. [[CrossRef](#)] [[PubMed](#)]
76. Lira, R.B.; Robinson, T.; Dimova, R.; Riske, K.A. Highly efficient protein-free membrane fusion: A giant vesicle study. *Biophys. J.* **2019**, *116*, 79–91. [[CrossRef](#)]
77. Somasundar, A.; Ghosh, S.; Mohajerani, F.; Massenburg, L.N.; Yang, T.; Cremer, P.S.; Velegol, D.; Sen, A. Positive and negative chemotaxis of enzyme-coated liposome motors. *Nat. Nanotechnol.* **2019**, *14*, 1129–1134. [[CrossRef](#)]
78. Bagatolli, L.A.; Needham, D. Quantitative optical microscopy and micromanipulation studies on the lipid bilayer membranes of giant unilamellar vesicles. *Chem. Phys. Lipids* **2014**, *181*, 99–120. [[CrossRef](#)] [[PubMed](#)]
79. Davidson, M.; Karlsson, M.; Sinclair, J.; Sott, K.; Orwar, O. Nanotube–Vesicle Networks with Functionalized Membranes and Interiors. *J. Am. Chem. Soc.* **2003**, *125*, 374–378. [[CrossRef](#)]
80. Jesorka, A.; Stepanyants, N.; Zhang, H.; Ortmen, B.; Hakonen, B.; Orwar, O. Generation of phospholipid vesicle-nanotube networks and transport of molecules therein. *Nat. Protoc.* **2011**, *6*, 791–805. [[CrossRef](#)]
81. Ali Doosti, B.; Fjällborg, D.; Kustanovich, K.; Jesorka, A.; Cans, A.S.; Lobovkina, T. Generation of interconnected vesicles in a liposomal cell model. *Sci. Rep.* **2020**, *10*, 14040. [[CrossRef](#)]
82. Wick, R.; Angelova, M.I.; Walde, P.; Luisi, P.L. Microinjection into giant vesicles and light microscopy investigation of enzyme-mediated vesicle transformations. *Chem. Biol.* **1996**, *3*, 105–111. [[CrossRef](#)]
83. Bucher, P.; Fischer, A.; Luisi, P.L.; Oberholzer, T.; Walde, P. Giant vesicles as biochemical compartments: The use of microinjection techniques. *Langmuir* **1998**, *14*, 2712–2721. [[CrossRef](#)]
84. Lefrançois, P.; Goudeau, B.; Arbault, S. Dynamic monitoring of a bi-enzymatic reaction at a single biomimetic giant vesicle. *Analyst* **2020**, *145*, 7922–7931. [[CrossRef](#)] [[PubMed](#)]
85. Foo, J.J.; Liu, K.K.; Chan, V. Thermal effect on a viscously deformed liposome in a laser trap. *Ann. Biomed. Eng.* **2003**, *31*, 354–362. [[CrossRef](#)]
86. Spyratou, E.; Mourelatou, E.A.; Georgopoulos, A.; Demetzos, C.; Makropoulou, M.; Serafetinides, A.A. Line optical tweezers: A tool to induce transformations in stained liposomes and to estimate shear modulus. *Colloids Surf. A Physicochem. Eng. Asp.* **2009**, *349*, 35–42. [[CrossRef](#)]
87. Ichikawa, M.; Yoshikawa, K. Optical transport of a single cell-sized liposome. *Appl. Phys. Lett.* **2001**, *79*, 4598–4600. [[CrossRef](#)]
88. Kulin, S.; Kishore, R.; Helmersson, K.; Locascio, L. Optical manipulation and fusion of liposomes as microreactors. *Langmuir* **2003**, *19*, 8206–8210. [[CrossRef](#)]
89. Inaba, T.; Ishijima, A.; Honda, M.; Nomura, F.; Takiguchi, K.; Hotani, H. Formation and maintenance of tubular membrane projections require mechanical force, but their elongation and shortening do not require additional force. *J. Mol. Biol.* **2005**, *348*, 325–333. [[CrossRef](#)]
90. Bolognesi, G.; Friddin, M.S.; Salehi-Reyhani, A.; Barlow, N.E.; Brooks, N.J.; Ces, O.; Elani, Y. Sculpting and fusing biomimetic vesicle networks using optical tweezers. *Nat. Commun.* **2018**, *9*, 1882. [[CrossRef](#)]
91. Shiomi, H.; Tsuda, S.; Suzuki, H.; Yomo, T. Liposome-based liquid handling platform featuring addition, mixing, and aliquoting of femtoliter volumes. *PLoS ONE* **2014**, *9*, e101820. [[CrossRef](#)]
92. Yoshino, T.; Yamaura, D.; Komiya, M.; Sugawara, M.; Mitsumori, Y.; Niwano, M.; Hirano-Iwata, A.; Edamatsu, K.; Sadgrove, M. Optical transport of sub-micron lipid vesicles along a nanofiber. *Opt. Express* **2020**, *28*, 38527–38538. [[CrossRef](#)]
93. Pong, M.; Umchid, S.; Guarino, A.J.; Lewin, P.A.; Litniewski, J.; Nowicki, A.; Wrenn, S.P. In vitro ultrasound-mediated leakage from phospholipid vesicles. *Ultrasonics* **2006**, *45*, 133–145. [[CrossRef](#)]
94. Dolatmoradi, A.; El-Zahab, B. Thermally-assisted ultrasonic separation of giant vesicles. *Lab Chip* **2016**, *16*, 3449–3453. [[CrossRef](#)] [[PubMed](#)]
95. Wang, X.; Tian, L.; Du, H.; Li, M.; Mu, W.; Drinkwater, B.W.; Han, X.; Mann, S. Chemical communication in spatially organized protocell colonies and protocell/living cell micro-arrays. *Chem. Sci.* **2019**, *10*, 9446–9453. [[CrossRef](#)] [[PubMed](#)]
96. Silva, G.T.; Tian, L.; Franklin, A.; Wang, X.; Han, X.; Mann, S.; Drinkwater, B.W. Acoustic deformation for the extraction of mechanical properties of lipid vesicle populations. *Phys. Rev. E* **2019**, *99*, 063002. [[CrossRef](#)] [[PubMed](#)]

97. Pereno, V.; Lei, J.; Carugo, D.; Stride, E. Microstreaming inside model cells induced by ultrasound and microbubbles. *Langmuir* **2020**, *36*, 6388–6398. [[CrossRef](#)] [[PubMed](#)]
98. Dimova, R.; Bezlyepkina, N.; Jordö, M.D.; Knorr, R.L.; Riske, K.A.; Staykova, M.; Vlahovska, P.M.; Yamamoto, T.; Yang, P.; Lipowsky, R. Vesicles in electric fields: Some novel aspects of membrane behavior. *Soft Matter* **2009**, *5*, 3201–3212. [[CrossRef](#)]
99. Korlach, J.; Reichle, C.; Müller, T.; Schnelle, T.; Webb, W.W. Trapping, deformation, and rotation of giant unilamellar vesicles in octode dielectrophoretic field cages. *Biophys. J.* **2005**, *89*, 554–562. [[CrossRef](#)]
100. Knorr, R.L.; Staykova, M.; Gracia, R.S.; Dimova, R. Wrinkling and electroporation of giant vesicles in the gel phase. *Soft Matter* **2010**, *6*, 1990–1996. [[CrossRef](#)]
101. Sugahara, K.; Morimoto, Y.; Takamori, S.; Takeuchi, S. A dynamic microarray device for pairing and electrofusion of giant unilamellar vesicles. *Sens. Actuators B Chem.* **2020**, *311*, 127922. [[CrossRef](#)]
102. Terasawa, H.; Nishimura, K.; Suzuki, H.; Matsuura, T.; Yomo, T. Coupling of the fusion and budding of giant phospholipid vesicles containing macromolecules. *Proc. Natl. Acad. Sci. USA* **2012**, *109*, 5942–5947. [[CrossRef](#)]
103. Miyakawa, S.; Uesugi, K.; Morishima, K. A Closed System for Pico-Liter Order Substance Transport from a Giant Liposome to a Cell. *Micromachines* **2018**, *9*, 331. [[CrossRef](#)]
104. Saito, A.C.; Ogura, T.; Fujiwara, K.; Murata, S.; Nomura, S.I.M. Introducing micrometer-sized artificial objects into live cells: A method for cell–giant unilamellar vesicle electrofusion. *PLoS ONE* **2014**, *9*, e106853. [[CrossRef](#)]
105. Desai, S.P.; Vahey, M.D.; Voldman, J. Electrically addressable vesicles: Tools for dielectrophoresis metrology. *Langmuir* **2009**, *25*, 3867–3875. [[CrossRef](#)] [[PubMed](#)]
106. Cui, Y.; Delaney, W.F.; Darroudi, T.; Wang, P. Microwave measurement of giant unilamellar vesicles in aqueous solution. *Sci. Rep.* **2018**, *8*, 497. [[CrossRef](#)] [[PubMed](#)]
107. Helfrich, W. Elastic properties of lipid bilayers: Theory and possible experiments. *Z. Nat. C* **1973**, *28*, 693–703. [[CrossRef](#)] [[PubMed](#)]
108. Ozeki, S.; Kurashima, H.; Abe, H. High-Magnetic-Field Effects on Liposomes and Black Membranes of Dipalmitoylphosphatidylcholin: Magnetoresponses in Membrane Potential and Magnetofusion. *J. Phys. Chem. B* **2000**, *104*, 5657–5660. [[CrossRef](#)]
109. Suzuki, K.; Toyota, T.; Sato, K.; Iwasaka, M.; Ueno, S.; Sugawara, T. Characteristic curved structure derived from collagen-containing tubular giant vesicles under static magnetic field. *Chem. Phys. Lett.* **2007**, *440*, 286–290. [[CrossRef](#)]
110. Bacri, J.C.; Cabuil, V.; Cebers, A.; Ménager, C.; Perzynski, R. Flattening of ferro-vesicle undulations under a magnetic field. *Europhys. Lett.* **1996**, *33*, 235–240. [[CrossRef](#)]
111. Veloso, S.R.; Andrade, R.G.; Castanheira, E.M. Magnetoliposomes: Recent advances in the field of controlled drug delivery. *Expert Opin. Drug Deliv.* **2021**, *18*, 1323–1334. [[CrossRef](#)]
112. Komatsu, D.; Fujiwara, K.; Nomura, S.I. Construction of a remote-controlled supramolecular micro-crawler. In *ECAL 2013: The Twelfth European Conference on Artificial Life*; MIT Press: Cambridge, MA, USA, 2013; pp. 208–209.
113. Li, Q.; Li, S.; Zhang, X.; Xu, W.; Han, X. Programmed magnetic manipulation of vesicles into spatially coded prototissue architectures arrays. *Nat. Commun.* **2020**, *11*, 232. [[CrossRef](#)]
114. Shahrubudin, N.; Lee, T.C.; Ramlan, R. An overview on 3D printing technology: Technological, materials, and applications. *Procedia Manuf.* **2019**, *35*, 1286–1296. [[CrossRef](#)]
115. Abele, T.; Messer, T.; Jahnke, K.; Hippler, M.; Bastmeyer, M.; Wegener, M.; Göpfrich, K. Two-Photon 3D Laser Printing Inside Synthetic Cells. *Adv. Mater.* **2022**, *34*, 2106709. [[CrossRef](#)] [[PubMed](#)]
116. Walther, T.; Jahnke, K.; Abele, T.; Göpfrich, K. Printing and Erasing of DNA-Based Photoresists Inside Synthetic Cells. *Adv. Funct. Mater.* **2022**, 2200762. [[CrossRef](#)]
117. Villar, G.; Graham, A.D.; Bayley, H. A tissue-like printed material. *Science* **2013**, *340*, 48–52. [[CrossRef](#)] [[PubMed](#)]
118. Mukwaya, V.; Mann, S.; Dou, H. Chemical communication at the synthetic cell/living cell interface. *Commun. Chem.* **2021**, *4*, 161. [[CrossRef](#)]